JACS
JOURNAL OF THE AMERICAN CHEMICAL SOCIETY

COMMUNICATION

pubs.acs.org/JACS

In Situ Measurements of the Formation and Morphology of Intracellular β-Amyloid Fibrils by Super-Resolution Fluorescence Imaging

Gabriele S. Kaminski Schierle,[†] Sebastian van de Linde,[‡] Miklos Erdelyi,[†,∥] Elin K. Esbjörner,[§] Teresa Klein,[‡] Eric Rees,[†] Carlos W. Bertoncini,[⊥] Christopher M. Dobson,[§] Markus Sauer,[*,‡] and Clemens F. Kaminski[*,†,¶]

[†]Department of Chemical Engineering and Biotechnology, University of Cambridge, Pembroke Street, Cambridge CB2 3RA, U.K.

[‡]Department of Biotechnology and Biophysics, Julius-Maximilians-University Würzburg, Am Hubland, 97074 Würzburg, Germany

[§]Department of Chemistry, University of Cambridge, Lensfield Road, Cambridge CB2 1EW, U.K.

[⊥]Laboratory of Molecular Biophysics, Institute for Research in Biomedicine, Baldiri Reixac 10-12, Barcelona, Spain

[∥]National Physics Laboratory, Hampton Road, Teddington TW11 0LW, U.K.

[¶]School of Advanced Optical Technologies, Friedrich Alexander University, D-91058 Erlangen, Germany

Supporting Information

ABSTRACT: Misfolding and aggregation of peptides and proteins is a characteristic of many neurodegenerative disorders, including Alzheimer's disease (AD). In AD the β-amyloid peptide (Aβ) aggregates to form characteristic fibrillar structures, which are the deposits found as plaques in the brains of patients. We have used direct stochastic optical reconstruction microscopy, *d*STORM, to probe the process of *in situ* Aβ aggregation and the morphology of the ensuing aggregates with a resolution better than 20 nm. We are able to distinguish different types of structures, including oligomeric assemblies and mature fibrils, and observe a number of morphological differences between the species formed *in vitro* and *in vivo*, which may be significant in the context of disease. Our data support the recent view that intracellular Aβ could be associated with Aβ pathogenicity in AD, although the major deposits are extracellular, and suggest that this approach will be widely applicable to studies of the molecular mechanisms of protein deposition diseases.

The pathological role of the β-amyloid (Aβ) peptide in Alzheimer's disease (AD) is one of the central questions in neurodegenerative research.[1] The formation of amyloid plaques in the extracellular space of the brain is one of the characteristics of patients who are in an advanced stage of the disease.[2] The Aβ peptide originates from the proteolytic processing of the transmembrane amyloid precursor protein (APP), and the resulting cleaved fragments constituting Aβ are predominantly 40 or 42 amino acids in length.[3] The 40-residue peptide, $A\beta_{1-40}$, is the most abundant form of Aβ in both healthy and AD brains and is considered to be less harmful than the second most common proteolytic product, the 42-residue peptide $A\beta_{1-42}$, which is strongly associated with disease.[4] $A\beta_{1-40}$ and $A\beta_{1-42}$ differ in their propensity to form cross-β structures, the latter being more aggregation prone, but both can readily form amyloid fibrils *in vitro* as well as precursor Aβ oligomers.[1,5] It is not yet well established which Aβ aggregation state prevails *in vivo*, nor is there a consensus on the precise subcellular location of its pathogenicity in the context of AD. β-amyloid plaques are typically found outside the cell, but considerable evidence is pointing toward a potential pathogenic relevance of intracellular Aβ accumulation.[6] Thus, peripherally inoculated β-amyloid-rich extracts have been shown to induce formation of amyloid deposits within the brains of APP transgenic mice, confirming that characteristics generally associated with prions are shared by other amyloidogenic polypeptides.[7] By analogy to the existence of prion strains, the presence of multiple aggregated forms of Aβ, known as fibril polymorphism, could contribute to variations in neurotoxicity and AD pathology.[8] A key step in understanding these phenomena lies in the ability to probe *in situ* the occurrence of amyloid aggregation in experimental models of disease.

Traditional high-resolution imaging techniques, such as electron microscopy (EM) and atomic force microscopy (AFM), have proved to be powerful for studying protein aggregation in excised tissue or *in vitro*.[9] Fluorescence techniques are, however, also developing rapidly and have recently been applied to studies of protein aggregation in a cellular context,[10] and highly specific and versatile labeling tools are now available for functional imaging using immunocytochemistry or fluorescent protein technology. These methods permit the spatial distribution of virtually every cellular substructure or protein to be analyzed in both fixed and living samples,[11] but in comparison to EM and AFM, their ability to characterize molecular species has until recently been limited by the fact that optical diffraction limits the obtainable spatial resolution to around 250 nm in the imaging plane, orders of magnitude larger than the size of typical biological macromolecular structures. The relatively recent development of optical super-resolution techniques, such as stimulated emission depletion (STED)[12] structured illumination (SIM),[13] and single-molecule localization and reconstruction techniques,[14] however, is beginning to bridge this resolution gap. Single-molecule localization techniques now routinely achieve a lateral resolution in the 20−30 nm range with variants including photoactivated localization microscopy (PALM), fluorescence

Received: March 3, 2011
Published: July 27, 2011

PALM (FPALM), stochastic optical reconstruction microscopy (STORM), and direct STORM (*d*STORM), all of which are powerful imaging methods that are comparably simple to implement. In the latter two approaches, increased spatial resolution is achieved by sequentially photoswitching individual fluorophores between a fluorescent on-state and a nonfluorescent off-state, which leads to a temporal separation of the individual fluorophores from an ensemble of emitters. The emission patterns are recorded on a wide-field fluorescence microscope equipped with a sensitive CCD camera, and the individual fluorophores can then be located precisely by fitting point spread functions (PSFs) to the measured photon distributions. As long as distinct emission patterns can be recorded for individual fluorophores (i.e., provided that recorded PSFs are spatially separated), the standard error of the fitted position can be minimized by increasing the number of photons collected, thus reducing noise.[15]

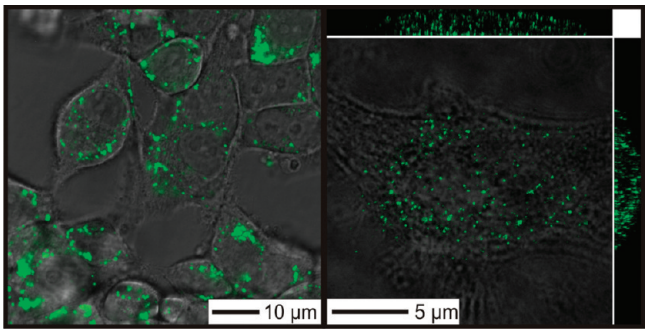

Figure 1. Ⓦ Extracellular Aβ_{1-40} is readily taken up by HeLa cells. (Left panel) Human HeLa cells were incubated with 0.5 μM HiLyte Fluor 488 Aβ_{1-40} for 1 h, washed, and imaged on a confocal microscope. (Right panel) The same cells were fixed with 4% paraformaldehyde prior to high-resolution imaging on a structured illumination microscope. The image shows a single *xy*-slice near the center of a cell containing Aβ_{1-40} (green), with a bright-field image superimposed. (Top and side panels) *xz* and *yz* maximum intensity projections of the stacks. The corresponding 3D distribution of intracellular HiLyte Fluor 488 Aβ_{1-40} inside the cell is shown in video 1 .

In the present study we used confocal fluorescence microscopy and SIM to investigate Aβ uptake when exogenously added to cells in culture, before applying *d*STORM[14c,e] to probe directly, with near nanometer resolution, the nature of the ensuing intracellular amyloid deposits formed by these peptides *in vivo*. In a first set of standard confocal fluorescence microscopy experiments we used HiLyte Fluor 488-labeled Aβ_{1-40} (Cambridge Bioscience, Bar Hill, UK) and showed that the Aβ peptide had been taken up by the cells within 1 h of incubation (Figure 1). We verified the intracellular location of Aβ_{1-40} using high-resolution, volume-resolved, SIM (see Figure 1, right panel and corresponding video 1, and SI). Similar studies were performed for SH-SY5Y cells (SI, Figure 1) and it was found that internalization is independent of whether the cell lines were neuronal

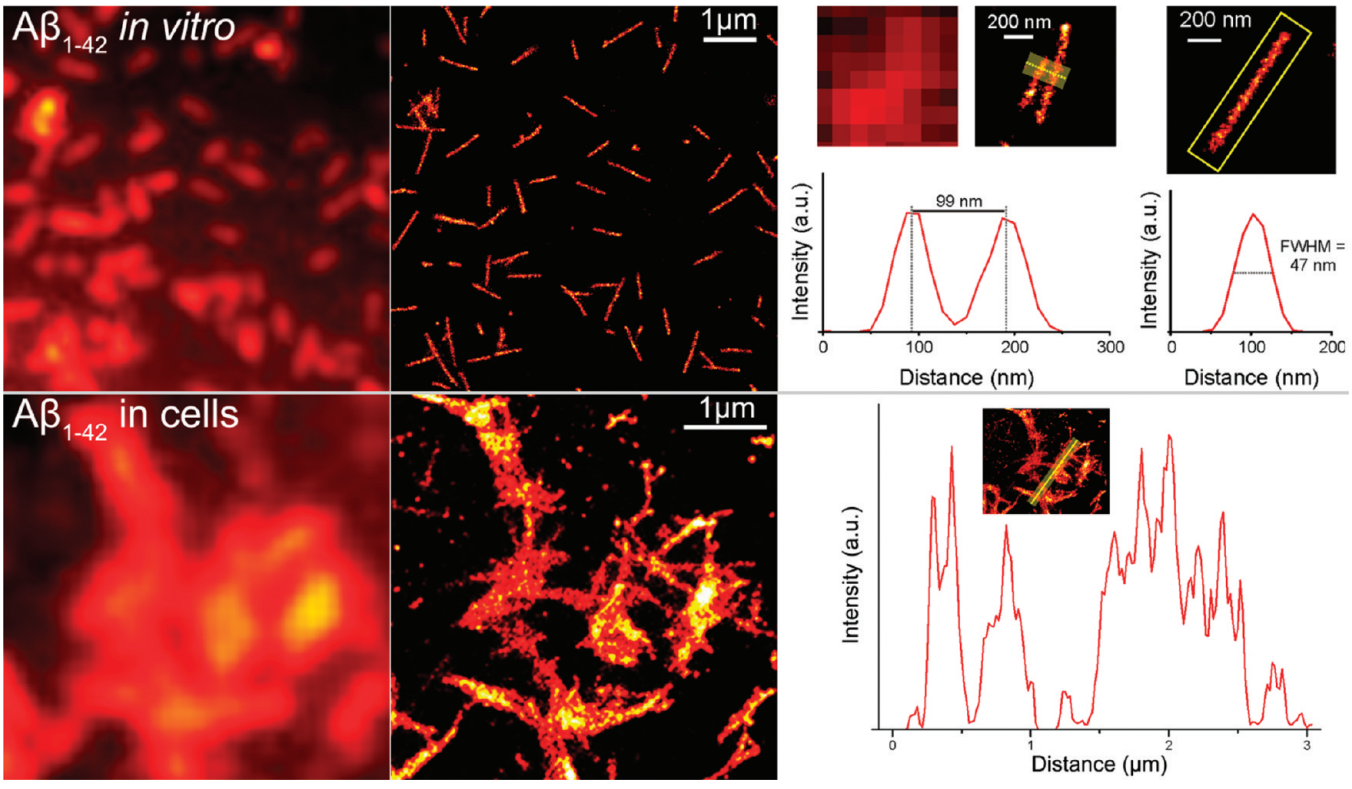

Figure 2. Ⓦ *d*STORM imaging permits the nature and morphology of intracellular Aβ_{1-42} aggregates to be probed in situ. **Top row** (Left): Fluorescence images of Aβ_{1-42} fibrils formed *in vitro* on the surface of a coverslip. (Center): *d*STORM image performed in TIRF mode corresponding to the fluorescence image on the left (see also video 2). (Right): Adjacent fibrils can be resolved well below the diffraction limit. Fibril diameters were determined to be in the 40−50 nm range from the full width half-maximum points of cross-sectional profiles. In addition to the actual fibril diameter, there is a significant contribution to this width from the size of fluorescent antibodies used in the immunochemical labeling procedure. **Bottom row** (Left and center): Fluorescence image and corresponding *d*STORM image of a section of a cell containing Aβ_{1-42} fibrils. *d*STORM was performed with highly inclined illumination (see Supporting Information [SI]). (Right): Intensity profile across a transverse section of a *d*STORM image displaying intracellular Aβ_{1-42} aggregates.

dx.doi.org/10.1021/ja201651w |*J. Am. Chem. Soc.* 2011, 133, 12902–12905

(SH-SY5Y cells) or non-neuronal (HeLa cells) in origin. We used FM4-64 as a marker for endocytotic vesicles to confirm the hypothesis that initially soluble and extracellular Aβ peptide becomes internalized and sorted into vesicles (SI, Figure 1). Previous studies have shown that Aβ species can accumulate in multivesicular bodies (MVBs) inside the cell,[6a,16] as well as in lysosomes and other vesicular compartments.[17] The compartmentalization into vesicles increases local Aβ concentrations and restricts the peptide to a confined space, factors known to favor intermolecular aggregation reactions.[18] There has been previous evidence that the loss of integrity of endosomal/lysosomal membranes represents an early event in Aβ pathogenesis,[19] and it has been suggested that leakage of intracellular vesicles may lead to Aβ-dependent cell death.[19] It is possible that the spontaneous growth of amyloid fibrils causes stress and even rupture of lysosomal membranes, leading to release of Aβ into the cytoplasm.

Figure 1 makes evident that the resolution provided by confocal fluorescence imaging and even structured illumination methods do not feature a sufficient spatial resolution to yield information on the morphology of the various Aβ species. Using super-resolution fluorescence imaging, however, we have been able to define important details of the intracellular aggregates that Aβ forms when exogenously added to cells in culture. One approach involved the use of direct labeling of Aβ_{1-40} with HiLyte Fluor 647 (a carbocyanine derivative) via an additional cysteine residue at the N-terminus. Another involved detection of unlabeled Aβ_{1-42} by means of a primary antibody reactive to residues, 1−17 in the Aβ peptide sequence (6E10, Covance, Leeds, UK) and a secondary antibody labeled with Alexa Fluor 647. In both cases we typically detected 1000−5000 photons per frame from single fluorophores, allowing a localization precision of better than 20 nm[15a] in the imaging plane, a limit determined experimentally from repetitive localizations of individual Alexa Fluor 647-labeled antibodies.

We first verified that *d*STORM is capable of resolving amyloid structures *in vitro*. Figure 2, top row, center panel, shows the morphology of small fibrillar structures present in a 390 μM stock solution of Aβ_{1-42}. A comparison with the image in the left panel, obtained with conventional imaging, demonstrates the dramatic resolution enhancement afforded by *d*STORM (see also video 2). These images were obtained in total internal reflection fluorescence (TIRF) mode to image fibrils immobilized on the sample coverslip. Our custom built *d*STORM microscope can also be operated in highly inclined illumination mode to permit imaging deep inside cells (see SI, Figures 2−5). We verified that *d*STORM is capable of resolving the morphology of Aβ_{1-42} aggregates *in situ*, deep inside cells (Figure 2, bottom row, and Figure 3 with corresponding video 3). The images were obtained from cells incubated for 1 h with a 0.5 μM solution of Aβ_{1-42}. The incubating medium was obtained by dilution from preconcentrated stock solutions containing both monomeric and aggregated species of Aβ_{1-42} (see SI, Figure 7, top row), and it is possible that both types are taken up by the cells. Upon dilution, no further aggregation took place and hence no further fibril growth was observed in the extracellular space. In contrast, within cells, larger and growing aggregates appeared already within one hour after incubation. (compare Figure 2, top and bottom rows, central panel). On the other hand, cells in contact with soluble Aβ_{1-40} showed at most small oligomeric species within the cells (SI, Figure 6).

The *d*STORM images were subjected to more detailed analysis in order to probe the morphology of the intracellular

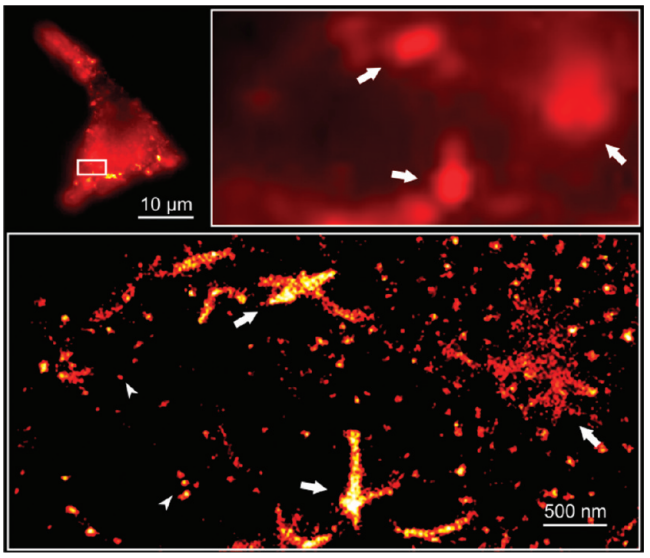

Figure 3. Ⓦ Super-resolution image of intracellular Aβ_{1-42} (see video 3). Fluorescence and corresponding *d*STORM images showing small oligomeric (arrow heads) and fibrillar (arrows) forms of Aβ_{1-42} formed within HeLa cells detected with a primary antibody against Aβ and a secondary antibody conjugated with Alexa Fluor 647. White rectangles on the three panels indicate the same field of view. Images were recorded in highly inclined illumination mode (see SI).

aggregates of Aβ. Cross sections of the fibrils show that the lateral resolution achieved by *d*STORM is sufficient to identify individual fibrils of Aβ_{1-42} both *in vitro* and *in vivo* (Figure 2) and reveal that intracellular fibrils have a similar morphology to that of fibrils observed *in vitro* (SI, Figure 7). In particular, intracellular fibrils show a multimodal distribution of lengths in the range between 0.3 and 1.9 μm (SI, Figure 8, left). The majority appear straight, but about 10% of the fibrils exhibit bending angles in the range 135 −165° (SI, Figure 8, right). These characteristics are similar to those observed for Aβ_{1-42} fibrils derived from the post mortem brains of AD patients.[20]

The *d*STORM images have substantially increased optical resolution relative to that characteristic of conventional imaging. The improvement in spatial resolution achieved with *d*STORM is demonstrated with single amyloid fibrils, since cross-sectional profiles (Figure 2, top row, far right) display distances between adjacent fibrils of less than 100 nm and apparent diameters of individual amyloid fibrils of 40−50 nm. Considering the size of the IgG antibodies (~ 8−10 nm) used to label the peptides, our data indicate that the diameters of individual fibrils, are ~20−30 nm, comparable to what is typically measured *in vitro* by TEM (SI, Figure 7). In addition, intracellular Aβ, as we report here, has been implicated in the formation of extracellular amyloid plaques.[16c] Our observations are furthermore in line with previous proposals that cytoplasmic aggregates contribute to Aβ pathogenicity.[6c]

Finally, the methodology described here offers a powerful approach to the study of misfolding and aggregation in a context that is of relevance for living systems. It is readily adapted for the investigation of other amyloidogenic proteins, such as α-synuclein, Tau and Huntingtin, and could, in addition to studies of the type discussed here, be used diagnostically to probe amyloid formation in tissue samples taken from patients. From a therapeutic point of view, a better understanding of the intracellular trafficking and fate of peptides associated with misfolding

disorders will undoubtedly pave the way for more effective intervention to treat or prevent these highly debilitating and rapidly proliferating conditions.

■ ASSOCIATED CONTENT

Supporting Information. Full description of experimental procedures, additional data, and complete ref 7a. The material is available free of charge via the Internet at http://pubs.acs.org.

■ AUTHOR INFORMATION

Corresponding Author
*cfk23@cam.ac.uk; m.sauer@uni-wuerzburg.de

■ ACKNOWLEDGMENT

We thank Alex Sossick and Dr. Nicola Lawrence for their help with OMX imaging and Dr. Alex Knight for stimulating discussions. This work was funded by a Wellcome Trust/MRC Strategic Award for Neurodegenerative Disorders (C.M.D. and C.F.K.). G. S.S.K. is supported by grants from the EPSRC and the Wellcome Trust. M.E. is funded by the EPSRC and acknowledges funding by the Hungarian National Office for Research and Technology OTKA Foundation. E.K.E. is supported by the Wenner-Gren foundation. C.W.B. is supported by an EU-FP7Marie Curie Fellowship. C.M.D. acknowledges funding by the BBSRC, and the Wellcome Trust. M.S. acknowledges funding by the Biophotonics Initiative of the BMBF (Bundesministerium für Bildung und Forschung), and C.F.K. by the EPSRC, the BBSRC, and the Wellcome Trust.

■ REFERENCES

(1) Haass, C.; Selkoe, D. J. *Nat. Rev. Mol. Cell. Biol.* **2007**, *8*, 101.
(2) Masters, C. L.; Simms, G.; Weinman, N. A.; Multhaup, G.; McDonald, B. L.; Beyreuther, K. *Proc. Natl. Acad. Sci. U.S.A.* **1985**, *82*, 4245.
(3) Kang, J.; Lemaire, H. G.; Unterbeck, A.; Salbaum, J. M.; Masters, C. L.; Grzeschik, K. H.; Multhaup, G.; Beyreuther, K.; Muller-Hill, B. *Nature* **1987**, *325*, 733.
(4) Kodali, R.; Wetzel, R. *Curr. Opin. Struct. Biol.* **2007**, *17*, 48.
(5) Glabe, C. G. *J. Biol. Chem.* **2008**, *283*, 29639.
(6) (a) Takahashi, R. H.; Milner, T. A.; Li, F.; Nam, E. E.; Edgar, M. A.; Yamaguchi, H.; Beal, M. F.; Xu, H.; Greengard, P.; Gouras, G. K. *Am. J. Pathol.* **2002**, *161*, 1869. (b) Oakley, H.; Cole, S. L.; Logan, S.; Maus, E.; Shao, P.; Craft, J.; Guillozet-Bongaarts, A.; Ohno, M.; Disterhoft, J.; Van Eldik, L.; Berry, R.; Vassar, R. *J. Neurosci.* **2006**, *26*, 10129. (c) Du, H.; Guo, L.; Fang, F.; Chen, D.; Sosunov, A. A.; McKhann, G. M.; Yan, Y.; Wang, C.; Zhang, H.; Molkentin, J. D.; Gunn-Moore, F. J.; Vonsattel, J. P.; Arancio, O.; Chen, J. X.; Yan, S. D. *Nat. Med.* **2008**, *14*, 1097. (d) Ren, P. H.; Lauckner, J. E.; Kachirskaia, I.; Heuser, J. E.; Melki, R.; Kopito, R. R. *Nat. Cell Biol.* **2009**, *11*, 219.
(7) (a) Meyer-Luehmann; et al. *Science* **2006**, *313*, 1781. (b) Eisele, Y. S.; Obermuller, U.; Heilbronner, G.; Baumann, F.; Kaeser, S. A.; Wolburg, H.; Walker, L. C.; Staufenbiel, M.; Heikenwalder, M.; Jucker, M. *Science* **2010**, *330*, 980.
(8) (a) Miller, Y.; Ma, B.; Nussinov, R. *Chem. Rev.* **2010**, *110*, 4820. (b) Kodali, R.; Williams, A. D.; Chemuru, S.; Wetzel, R. *J. Mol. Biol.* **2010**, *401*, 503.
(9) Dobson, C. M. *Nature* **2003**, *426*, 884.
(10) (a) Dai, X. W.; Eccleston, M. E.; Yue, Z. L.; Slater, N. K. H.; Kaminski, C. F. *POLYMER* **2006**, *47*, 2689. (b) Roberti, M. J.; Bertoncini, C. W.; Klement, R.; Jares-Erijman, E. A.; Jovin, T. M. *Nat. Methods* **2007**, *4*, 345. (c) Meyer-Luehmann, M.; Spires-Jones, T. L.; Prada, C.; Garcia-Alloza, M.; de Calignon, A.; Rozkalne, A.; Koenigsknecht-Talboo, J.; Holtzman, D. M.; Bacskai, B. J.; Hyman, B. T. *Nature* **2008**, *451*, 720. (d) Roberti, M. J.; Morgan, M.; Menendez, G.; Pietrasanta, L. I.; Jovin, T. M.; Jares-Erijman, E. A. *J. Am. Chem. Soc.* **2009**, *131*, 8102. (e) van Ham, T. J.; Esposito, A.; Kumita, J. R.; Hsu, S. T.; Kaminski Schierle, G. S.; Kaminski, C. F.; Dobson, C. M.; Nollen, E. A.; Bertoncini, C. W. *J. Mol. Biol.* **2010**, *395*, 627. (f) Chan, F. T. S.; Kaminski, C. F.; Kaminski Schierle, G. S. *ChemPhysChem* **2011**, *12*, 500. (g) Kaminski Schierle, G. S.; Bertoncini, C. W.; Chan, F. T. S.; van der Goot, A. T.; Schwedler, S.; Skepper, J.; Schlachter, S.; van Ham, T.; Esposito, A.; Kumita, J. R.; Nollen, E. A. A.; Dobson, C. M.; Kaminski, C. F. *ChemPhysChem* **2011**, *12*, 673.
(11) (a) Conchello, J. A.; Lichtman, J. W. *Nat. Methods* **2005**, *2*, 920. (b) Giepmans, B. N.; Adams, S. R.; Ellisman, M. H.; Tsien, R. Y. *Science* **2006**, *312*, 217.
(12) Hell, S. W. *Science* **2007**, *316*, 1153.
(13) Kner, P.; Chhun, B. B.; Griffis, E. R.; Winoto, L.; Gustafsson, M. G. *Nat. Methods* **2009**, *6*, 339.
(14) (a) Betzig, E.; Patterson, G. H.; Sougrat, R.; Lindwasser, O. W.; Olenych, S.; Bonifacino, J. S.; Davidson, M. W.; Lippincott-Schwartz, J.; Hess, H. F. *Science* **2006**, *313*, 1642. (b) Huang, B.; Wang, W.; Bates, M.; Zhuang, X. *Science* **2008**, *319*, 810. (c) Heilemann, M.; van de Linde, S.; Schuttpelz, M.; Kasper, R.; Seefeldt, B.; Mukherjee, A.; Tinnefeld, P.; Sauer, M. *Angew. Chem., Int. Ed.* **2008**, *47*, 6172. (d) Vogelsang, J.; Cordes, T.; Forthmann, C.; Steinhauer, C.; Tinnefeld, P. *Proc. Natl. Acad. Sci. U.S.A.* **2009**, *106*, 8107. (e) Wombacher, R.; Heidbreder, M.; van de Linde, S.; Sheetz, M. P.; Heilemann, M.; Cornish, V. W.; Sauer, M. *Nat. Methods* **2010**, *7*, 717. (f) Patterson, G.; Davidson, M.; Manley, S.; Lippincott-Schwartz, J. *Annu. Rev. Phys. Chem.* **2010**, *61*, 345.
(15) (a) Thompson, R. E.; Larson, D. R.; Webb, W. W. *Biophys. J.* **2002**, *82*, 2775. (b) Yildiz, A.; Forkey, J. N.; McKinney, S. A.; Ha, T.; Goldman, Y. E.; Selvin, P. R. *Science* **2003**, *300*, 2061.
(16) (a) Langui, D.; Girardot, N.; El Hachimi, K. H.; Allinquant, B.; Blanchard, V.; Pradier, L.; Duyckaerts, C. *Am. J. Pathol.* **2004**, *165*, 1465. (b) Almeida, C. G.; Takahashi, R. H.; Gouras, G. K. *J. Neurosci.* **2006**, *26*, 4277. (c) Friedrich, R. P.; Tepper, K.; Ronicke, R.; Soom, M.; Westermann, M.; Reymann, K.; Kaether, C.; Fandrich, M. *Proc. Natl. Acad. Sci. U.S.A.* **2010**, *107*, 1942.
(17) (a) Nixon, R. A. *J. Cell Sci.* **2007**, *120*, 4081. (b) Shie, F. S.; LeBoeuf, R. C.; Jin, L. W. *Neuroreport* **2003**, *14*, 123. (c) Ling, D.; Song, H. J.; Garza, D.; Neufeld, T. P.; Salvaterra, P. M. *PLoS One* **2009**, *4*, e4201.
(18) (a) Gorman, P. M.; Yip, C. M.; Fraser, P. E.; Chakrabartty, A. *J. Mol. Biol.* **2003**, *325*, 743. (b) Lomakin, A.; Teplow, D. B.; Kirschner, D. A.; Benedek, G. B. *Proc. Natl. Acad. Sci. U.S.A.* **1997**, *94*, 7942.
(19) Yang, A. J.; Chandswangbhuvana, D.; Margol, L.; Glabe, C. G. *J. Neurosci. Res.* **1998**, *52*, 691.
(20) Paravastu, A. K.; Qahwash, I.; Leapman, R. D.; Meredith, S. C.; Tycko, R. *Proc. Natl. Acad. Sci. U.S.A.* **2009**, *106*, 7443.